Communication

Formation of Gold–Methanethiyl Self-Assembled Monolayers

Yun Wang, Noel S. Hush, and Jeffrey R. Reimers

J. Am. Chem. Soc., **2007**, 129 (47), 14532-14533 • DOI: 10.1021/ja0743442

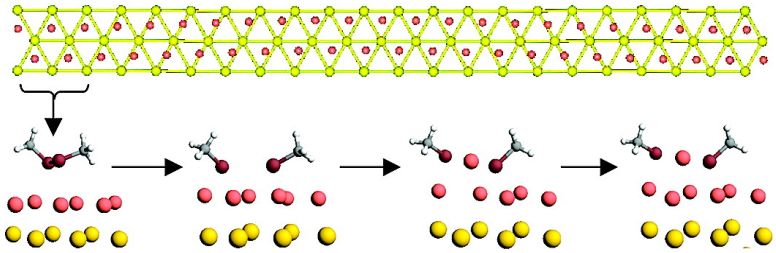

More About This Article

Additional resources and features associated with this article are available within the HTML version:

- Supporting Information
- Links to the 5 articles that cite this article, as of the time of this article download
- Access to high resolution figures
- Links to articles and content related to this article
- Copyright permission to reproduce figures and/or text from this article

View the Full Text HTML

J|A|C|S
COMMUNICATIONS

Published on Web 11/08/2007

Formation of Gold−Methanethiyl Self-Assembled Monolayers

Yun Wang,[†] Noel S. Hush,[†,‡] and Jeffrey R. Reimers*[,†]

School of Chemistry and School of Molecular and Microbial Biosciences, The University of Sydney, NSW 2006, Australia

Received June 15, 2007; E-mail: reimers@chem.usyd.edu.au

Self-assembled monolayers (SAMs) may be useful in next-generation electronic devices as ordered organic layers tailor surface properties.[1,2] Thiol−gold SAMs, formed by exposing thiols or disulfides to Au(111), are the most studied systems, owing to their stability and highly ordered structures. However, surface pitting can occur, and the surface chemistry is clearly very complex.[3−8] We consider the properties of the iconic shortest SAM that formed by chemisorbed methanethiyl radicals $CH_3S^{\bullet}$. Scanning tunneling microscopy (STM) experiments[1] indicate that the initial chemisorption of dimethyldisulfide (DMDS) on the gold (22 × $\sqrt{3}$) reconstructed Au(111) surface proceeds without surface pitting. At moderate coverage the surface reconstruction is lifted and surface pitting sets in, until a regular (1 × 1) hexagonal monolayer lattice appears. Since in the reconstructed surface 46 atoms occupy 44 bulklike positions, forming two rows of 23 atoms along the $\langle 1\bar{1}0 \rangle$ direction (see Figure 1a),[9,10] SAM production involves a significant surface transformation.[1,3,6,11]

At monolayer coverage, gold adatoms sitting above the regular unreconstructed Au(111) surface have been implicated in the SAM structure;[3,6,11] this motif, shown in Figure 1e, we name AD/UNRECON. Yu et al. suggested that sulfur atoms bond to Au adatoms on the basis of normal incidence X-ray standing wave (NIXSW) spectroscopic measurements,[11] while Maksymovych et al. interpreted STM images as indicating that DMDS molecules dissociatively adsorb through gold−adatom-mediated bonds.[3] Further, Mazzarello et al. used density-functional theory (DFT) calculations to predict that a DMDS molecule could draw an Au(111) atom from the surface layer to form a stable chemisorbed species with a nearby surface vacancy;[6] this novel structure we name ADVAC/UNRECON. Its properties were consistent with the results from their photoelectron diffraction (PED) and grazing incidence X-ray diffraction (GIXRD) measurements.[6]

We use DFT calculations to model the formation of the AD/UNRECON structure commencing with exposure of the clean reconstructed surface to either DMDS or methanethiol (CH_3SH). We predict the coverage at which the reconstruction is lifted.

All computations are performed using the Vienna ab initio simulation package (VASP).[12] Electron-ion interactions are described using the ultrasoft pseudopotentials.[13,14] A plane-wave basis set is employed with a kinetic energy cutoff of 300 eV. For the electron−electron exchange and correlation interactions, the functional of Perdew and Wang (PW91),[15] a form of the general gradient approximation (GGA), is used throughout. The Au(111) surface is modeled by a supercell comprising a four-layer slab separated by a vacuum region of six-layer equivalent thickness. When the geometry is optimized, the top two atomic layers and the adsorbates are relaxed, while the lower two layers are fixed at their ideal bulklike position.[16] The structure of the reconstructed Au(111) (22 × $\sqrt{3}$) surface is taken from previous calculations.[17] The methods of Neugebauer and Makov et al. are used to correct for the surface dipole moment.[18,19] We perform Brillouin-zone integrations using Monkhorst−Pack grids of special points: (4 × 6 × 1) and (1 × 4 × 1) *k*-points meshes are employed for the (3 × $\sqrt{3}$) and (22 × $\sqrt{3}$) surface cells, respectively. The *k*-points meshes in our calculation are sufficient for our purposes.[17,20]

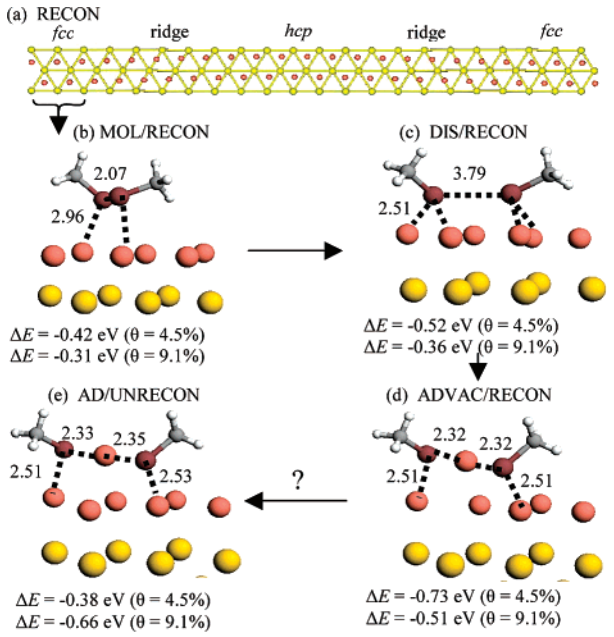

Figure 1. Stages in the adsorption of DMDS on the (22 × $\sqrt{3}$) reconstructed Au(111) surface: (a) one unit cell of the bare surface and subsurface layers, showing the fcc, hcp, and ridge domains, (b) the initial molecular physisorbed state MOL/RECON on atoms sampled from the fcc domain, (c) the subsequent dissociated state DIS/RECON, (d) after a gold is extracted from the fcc domain to form a molecule-attached adatom and associated surface vacancy ADVAC/RECON, and (e) after unreconstruction of the surface to eliminate the vacancy AD/UNRECON. Key bond lengths, in Å, are shown, while ΔE is the adsorption energy of DMDS at a coverage of θ sulfur atoms per gold atom on the unreconstructed surface: yellow, subsurface gold; pink, surface and adatom gold; brown, sulfur.

The (22 × $\sqrt{3}$) reconstruction of the Au(111) surface pushes Au atoms sideways along the $\langle 11\bar{2} \rangle$ direction away from the usual fcc sites occupied by the surface layer toward the higher-energy hcp sites.[10,17] In doing so, some gold atoms are forced to occupy even higher-energy bridge sites, thus raising above the surface. As a result, the surface displays apparent grain boundary ridges between fcc-like and hcp-like valleys, see Figure 1a. We investigate the adsorption properties of DMDS on both the fcc and hcp domains of the reconstructed surface at the low coverages of θ = 4.5% S atoms per Au surface atom (n = 1 DMDS molecule per (22 × $\sqrt{3}$) cell) and θ = 9.1% (n = 2); monolayer coverage is much higher, θ = 33.3%. The strongest adsorption is found for the fcc domain, in agreement with experiment,[17,21] and for this Figure 1 shows the details of the structure and the average adsorption energy of a DMDS molecule on the reconstructed surface is

[†] School of Chemistry, The University of Sydney.
[‡] School of Molecular and Microbial Biosciences, The University of Sydney.

10.1021/ja0743442 CCC: $37.00

$$\Delta E = (E_{total} - E_{recon-surface} - nE_{DMDS})/n$$

for MOL/RECON, DIS/RECON, and ADVAC/RECON, and

$$\Delta E = (E_{total} - E_{recon-surface} - nE_{DMDS} - (2-n)E_{Au-bulk})/n$$

for AD/UNRECON. Note that the calculated energy for adatom formation on the clean surface is $(E_{recon-surface} - 2E_{Au-bulk} - E_{unrecon-surface})/2 = 0.43$ eV.[17] Initially DMDS physisorbes as a molecule on the fcc domain of the reconstructed surface in a structure named MOL/RECON (Figure 1b) with, for $\theta = 4.5\%$, $\Delta E = -0.42$ eV. The molecule then dissociates to form two adsorbed methanethiyl radicals in structure DIS/RECON (Figure 1c, $\Delta E = -0.52$ eV) and then abstracts a gold atom from the fcc domain leaving a nearby surface vacancy to form the structure ADVAC/RECON (Figure 1d, $\Delta E = -0.73$ eV). At $\theta = 4.5\%$, lifting the reconstruction to produce the AD/UNRECON structure (Figure 1e, $\Delta E = -0.38$ eV) is endothermic by 0.35 eV, becoming exothermic by 0.15 eV at $\theta = 9.1\%$. On the hcp domain, the physisorption energy at $\theta = 4.5\%$ is only $\Delta E = -0.24$ eV, dissociation is endothermic by 0.01 eV, and the final ADVAC/RECON structure has an energy of only $\Delta E = -0.66$ eV. The fcc/hcp differences are greatest for the DIS/RECON configuration and arise as the S atom is near an unfavorable top site above the hcp domain compared to a favorable fcc/bridge site above the fcc domain.[4,7,8]

Most significantly, the calculated AD/UNRECON structure (Figure 1e) has very similar properties to those observed[22] for the high-coverage SAM structure: the S atoms sit on top sites of the Au(111) surface at 2.54 Å separation, in agreement with the experimental value of 2.50 ± 0.05 Å.[22] The ADVAC/RECON structure also has similar properties and resembles previous DFT predictions[6] of the transient ADVAC/UNRECON structure.

Calculations at a range of coverages up to half monolayer indicate that the binding of $CH_3SAuSCH_3$ to the unreconstructed surface is coverage-independent. Using this result, the effect of coverage on the driving force for lifting the surface reconstruction is modeled, and the process

$$n\text{ADVAC/RECON} \rightarrow n\text{AD/UNRECON} + (2-n)\text{Au}_{bulk}$$

is predicted to be exothermic above $n = 1.6$, implying a coverage of $\theta = 7.8\%$ (one S per 13 unreconstructed-surface Au atoms). This is consistent with the computed results for $n = 1$ (4.5% reconstruction remains) and $n = 2$ (9.1%, reconstruction lifted).

For the direct adsorption of DMDS on the unreconstructed Au(111) surface we used a $(3 \times \sqrt{3})$ surface cell (at monolayer coverage, $\theta = 33.3\%$) and obtained very similar results to those previously reported.[4,5,8,23] The analogous energies to the MOL/RECON, DIS/RECON, and ADVAC/RECON structures at $\Delta E = -0.42$, -0.52, and -0.73 eV are -0.16, -0.34, and -0.42 eV, respectively, indicating that the adsorbate binds more strongly to the reconstructed surface. However, it is also clear that once the surface reconstruction is lifted, monolayer growth continues via surface adatom/vacancy formation. Hence, as vacancies are chemically more active than flat terraces,[21] surface pits form.[1,10,24]

Methanethiyl SAMs are also formed on exposure of the reconstructed surface to methanethiol. Calculated structures and energies for the physisorbed MOL/RECON and ADVAC/RECON configurations are shown in Figure 2, structures a and b, respectively. While the physisorbed structure is strongly bound at $\Delta E = -0.51$ eV, the ADVAC/RECON structure is endothermic at $\Delta E = 0.18$ eV. Similarly, the ADVAC/UNRECON structure is endothermic by 0.29 eV on the unreconstructed surface. The mechanism

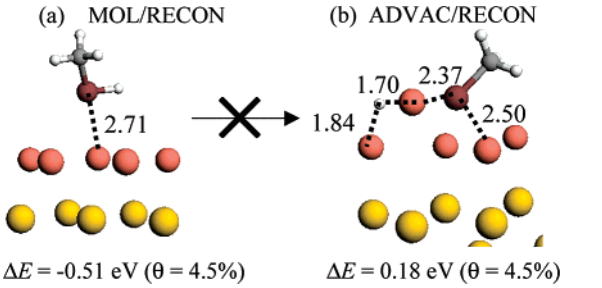

Figure 2. The configuration of (a) molecular physisorption and (b) dissociated adatom/vacancy binding of methanelthiol on the fcc domain of the $(22 \times \sqrt{3})$ reconstructed Au(111) surface. Key bond lengths, in Å, are shown: yellow, subsurface gold; pink, surface and adatom gold; brown, sulfur.

for monolayer growth for thiol adsorption thus must be quite different to that for disulfide adsorption, which is supported by the recent experimental observations that S−H bonds of methanethiols are merely broken, assisted by surface defects.[7,21]

In summary, we show that (i) the reconstructed surface is more reactive to thiols and disulfides than is the unreconstructed one, (ii) that its fcc domain is the most reactive; (iii) that DMDS adsorption leads to adatom/vacancy formation on the reconstructed surface, (iv) that above $\theta = 7.8\%$ the surface vacancies are eliminated through lifting the reconstruction, (v) that subsequent adsorption proceeds through adatom/vacancy formation on the unreconstructed surface leading to surface pit formation, and (vi) that thiol chemisorption proceeds via a different mechanism.

Acknowledgment. We thank the Australian Research Council for funding this work and the Australia Partnership for Advanced Computing (APAC) for computational resources.

References

(1) Vericat, C.; Vela, M. E.; Salvarezza, R. C. *Phys. Chem. Chem. Phys.* **2005**, *7*, 3258.
(2) Love, J. C.; Estroff, L. A.; Kriebel, J. K.; Nuzzo, R. G.; Whitesides, G. M. *Chem. Rev.* **2005**, *105*, 1103.
(3) Maksymovych, P.; Sorescu, D. C.; Yates, J. T., Jr. *Phys. Rev. Lett.* **2006**, *97*, 146103.
(4) Maksymovych, P.; Sorescu, D. C.; Yates, J. T. *J. Phys. Chem. B* **2006**, *110*, 21161.
(5) Danisman, M. F.; Casalis, L.; Bracco, G.; Scoles, G. *J. Phys. Chem. B* **2002**, *106*, 11771.
(6) Mazzarello, R.; Cossaro, A.; Verdini, A.; Rousseau, R.; Casalis, L.; Danisman, M. F.; Floreano, L.; Scandolo, S.; Morgante, A.; Scoles, G. *Phys. Rev. Lett.* **2007**, *98*, 16102.
(7) Zhou, J. G.; Hagelberg, F. *Phys. Rev. Lett.* **2006**, *97*, 45505.
(8) Vargas, M. C.; Giannozzi, P.; Selloni, A.; Scoles, G. *J. Phys. Chem. B* **2001**, *105*, 9509.
(9) Min, B. K.; Alemozafar, A. R.; Biener, M. M.; Biener, J.; Friend, C. M. *Top. Catal.* **2005**, *36*, 77.
(10) Zhang, J.; Chi, Q.; Ulstrup, J. *Langmuir* **2006**, *22*, 6203.
(11) Yu, M.; Bovet, N.; Satterley, C. J.; Bengio, S.; Lovelock, K. R. J.; Milligan, P. K.; Jones, R. G.; Woodruff, D. P.; Dhanak, V. *Phys. Rev. Lett.* **2006**, *97*, 166102.
(12) Kresse, G.; Hafner, J. *Phys. Rev. B* **1993**, *47*, RC558.
(13) Vanderbilt, D. *Phys. Rev. B* **1990**, *41*, 7892.
(14) Kresse, G.; Hafner, J. *J. Phys. Condens. Matter* **1994**, *6*, 8245.
(15) Perdew, J. P.; Wang, Y. *Phys. Rev. B* **1992**, *45*, 13244.
(16) Bilić, A.; Reimers, J. R.; Hush, N. S.; Hafner, J. *J. Chem. Phys.* **2002**, *116*, 8981.
(17) Wang, Y.; Hush, N. S.; Reimers, J. R. *Phys. Rev. B* **2007**, *75*, 233416.
(18) Neugebauer, J.; Scheffler, M. *Phys. Rev. B* **1992**, *46*, 16067.
(19) Makov, G.; Payne, M. C. *Phys. Rev. B* **1995**, *51*, 4014.
(20) Bilić, A.; Reimers, J. R.; Hush, N. S. *J. Chem. Phys.* **2005**, *122*, 094708.
(21) Rzeźnicka, I. I.; Lee, J. S.; Maksymovych, P.; Yates, J. T. *J. Phys. Chem. B* **2005**, *109*, 15992.
(22) Kondoh, H.; Iwasaki, M.; Shimada, T.; Amemiya, K.; Yokoyama, T.; Ohta, T. *Phys. Rev. Lett.* **2003**, *90*, 066102.
(23) Nuzzo, R. G.; Zegarski, B. R.; Dubois, L. H. *J. Am. Chem. Soc.* **1987**, *109*, 733.
(24) Poirier, G. E. *Langmuir* **1997**, *13*, 2019.

JA0743442